Shear Stiffness of Notched Connectors in Glue Laminated Timber-Concrete Composite Beams Under Fire Conditions

Danrong Shi,[a] Xiamin Hu,[a,]* Jing Zhang,[a] and Hao Du [b]

Shear connectors ensure effective interaction between wood beams and concrete slabs of composite beams, and their properties noticeably affect the fire resistance of timber-concrete composite beams. To investigate the shear stiffness of notched connectors in glued laminated timber (GLT)-concrete composite beams under fire conditions, 16 shear tests were conducted. The effects of fire duration and notch length on shear properties of the connectors for a given spacing were studied. The fire tests indicated that the reduction of the notch length from 200 mm to 150 mm remarkably affected the failure mode of the shear specimens, changing from compression failure of notched wood to shear failure of notched concrete. The increase in fire duration reduced effective width of the notched wood, negatively affected the shear stiffness and shear capacity of the connectors, and the shear stiffness decreased more rapidly. The notch length did not have a substantial effect on the shear stiffness of connectors. Based on the experimental results, an analytical model to estimate the shear stiffness of notched connectors in GLT-concrete beam under fire conditions was established.

DOI: 10.15376/biores.17.4.6397-6410

Keywords: GLT-concrete composite beams; Notched connectors; Shear stiffness; ISO fire; Analytical model

Contact information: a: College of Civil Engineering, Nanjing Tech University, Nanjing 211816 China; b: College of Civil Engineering, Nanjing Forestry University, Nanjing 210037 China;
** Corresponding author: huxm_njtech@163.com*

INTRODUCTION

A timber-concrete composite (TCC) beam typically consists of a bottom wood member in the tensile zone, a top concrete slab in the compression zone, and the connector between the two members. Through replacing the timber on the top of traditional wood structures with concrete slabs, composite beams with larger strength and stiffness (Ceccotti 2002), better sound insulation (Zhang *et al.* 2020c), better vibration comfort (Xie *et al.* 2020), and better fire performance (Du *et al.* 2021a) are achieved.

The bending tests of TCC beam performed by Yeoh *et al.* (2011a), Du *et al.* (2021b), and Jiang and Crocetti (2019) at room temperature show that shear connectors in TCC beams are essential in providing high composite action between timber beam and concrete slab. The most frequently used shear connectors are steel connectors, such as steel bars (Djoubissie *et al.* 2018), steel dowels (Dias *et al.* 2007), lag screws (Du *et al.* 2019, 2020), steel-toothed plates (Yeoh *et al.* 2011b), and self-tapping screws (Kavaliauskas *et al.* 2007; Zhang *et al.* 2020a). The notched connectors (Yeoh *et al.* 2008) and hybrid connectors (Marchi and Pozza 2021) are also used for TCC beams. However, notched connectors and steel-toothed plate commonly have higher stiffness and bearing capacity than dowel-type fasteners (Ceccotti 2002; Dias and Jorge 2011).

The notched connectors are formed by cutting grooves on wood and then filling them with concrete, which are usually considered one of the most effective and cost-optimal shear connectors in TCC beams. The high stiffness of notched connectors mainly comes from the compression area between wood and concrete on the effective bearing surface (Zhang *et al.* 2022a). If the notch is used as the main connector to provide most of the shear stiffness, and the screw is used as the auxiliary connector to improve the connector ductility, the advantages of the two connectors in mechanical properties are effectively exerted.

Thus far, researchers have conducted extensive experiments on the shear stiffness of notched connectors in TCC beams at room temperature. Zhang *et al.* (2020b) tested 10 types of notched connectors in glued laminated timber (GLT)-concrete composite beams under shear, varying with timber sheared length, notch dimensions, timber orientation, and self-tapping screw location. Test results showed that notched connectors with wood parallel-to-grain had higher stiffness than self-tapping screws and the connectors with wood perpendicular-to-grain. The notch depth positively affected the shear stiffness of the connectors, whereas the effect of timber sheared length was negligible. Yeoh *et al.* (2008, 2011b) performed shear tests to investigate triangular, dove-tail, and rectangular notched connectors in laminated veneer lumber (LVL)-concrete composite beams. A total of 12 shear specimens were fabricated with varying factors including notch depth, notch length, lag screw diameter, screw embedment depth, and existence of screws that were tested to examine the shear properties of notched connectors. Test data suggested that the shear stiffness of triangular notched connectors was lower than that of rectangular notches when the compression areas of two notches were similar. The presence of lag screws allowed the connector to maintain good stiffness after reaching the serviceability limit state and provided ductility after peak load, whereas screw diameter ranging between 12 and 16 mm only slightly affected the connectors shear stiffness. Shi *et al.* (2022a) presented test results of an experimental study of notched connectors in GLT-concrete composite beams, varying the loading method, screw number, notch width, and additional reinforcement screw. Test results showed that notch width was the most important factor that affected the shear stiffness of connectors, whereas other factors had little effect on shear stiffness of connectors.

However, the information available on shear stiffness of connectors in TCC beams after fire is limited. Fontana and Frangi (1999) investigated the shear behavior of notched connectors with glued dowels, and inclined screw connectors in TCC beams under International Organization for Standardization (ISO) fire. A total of 12 composite specimens with varying dimensions of timber section, type of wood, and fire duration were designed and tested under shear. Test data indicated that because of the high stiffness of notched connectors, and the presence of the glued dowels, no loss of shear stiffness of notched connectors was observed in the tests. An increase in temperature of wood near the screw negatively impacted the stiffness of inclined screw connectors. Frangi *et al.* (2010) theoretically analyzed the shear properties of inclined screw connectors in TCC beams under ISO fire. Two methods were proposed to determine the stiffness of screw connectors. The first one was effective cross-section method, which considered the relationship between wood stiffness and temperature. The other one was established to a simplified calculation method based on fire test results to calculate the stiffness of connectors through the modification factor $k_{\text{mod, fi}}$.

The main aim of this study was to investigate the important parameters that may affect the shear stiffness of notched connectors under fire. This was studied by fabricating and testing 16 shear specimens for a given connector, notch, spacing. The connectors with three different notch lengths were shear tested at room temperature and after the same fire duration to investigate the impact of notch length on connector shear stiffness. The connectors with the same notch length under different fire exposure times were shear tested as well to study the influence of fire duration on connector shear stiffness. The serviceability shear stiffness, load-slip relationship, and failure modes of connectors at room temperature and after fire were studied. Based on experimental results and calculation method at room temperature, an analytical model for shear stiffness of notched connectors under fire is proposed. The results and calculation method in this study will offer reference for the structural design and development of notched connectors in GLT-concrete composite beams under fire.

EXPERIMENTAL

Materials, Specimen Design, and Testing Methods

Shear specimens

Sixteen specimens were designed following literature methods (Dias *et al.* 2018; Auclair 2020) and fabricated into eight groups. The shear specimen had a GLT beam length l_t of 1300 mm, a width b_t of 150 mm, and a height h_t of 300 mm. The concrete slab of the specimen was 1500 mm in length l_c, 400 mm in width b_c, and 80 mm in thickness h_c. The timber sheared length l_{es}, the notch width b_n, and the notch depth t_n, were respectively 550, 150, and 40 mm. A plywood with a thickness h_b of 15 mm was used as a formwork between the concrete slab and the wood beam. Under fire conditions, the plywood could effectively slow down the heating of the concrete slab. A lag screw with an overall length of 195 mm was vertically embedded into the notch, which had an embedment length of 80 mm in the GLT beam and 60 mm in the concrete slab. A single-layer, bidirectional steel mesh with a diameter of 10 mm and a spacing of 150 mm was installed in the intermediate of the concrete slab. A schematic view of the shear specimen is shown in Fig. 1. The variation among the specimens was notch length l_n and fire duration t, as displayed in Table 1. The specimens were named according to their materials, notch length, and exposure time, where G denotes GLT, C denotes concrete, N denotes notched connectors, AT denotes room temperature, and ET denotes fire conditions. For example, GCN200-ET45 represents GLT-concrete composite shear specimens with the notch length of 200 mm, and exposed to fire for 45 min.

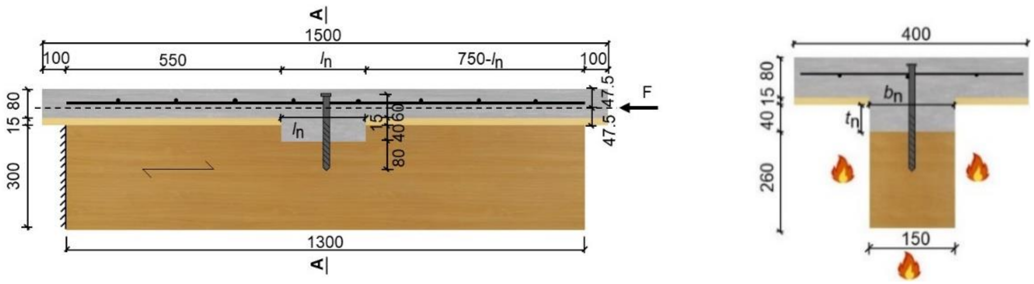

a) b)

Fig. 1. Schematic view of the shear specimen (unit: mm): a) longitudinal section; and b) transverse section of A-A

Table 1. Variations of Specimens in Shear Tests

Specimen Group	Number of Specimens	Notch Length l_n (mm)	Fire Duration t (min)
GCN150-AT	2	150	0
GCN200-AT	2	200	0
GCN250-AT	2	250	0
GCN150-ET45	2	150	45
GCN200-ET45	2	200	45
GCN250-ET45	2	250	45
GCN200-ET30	2	200	30
GCN200-ET60	2	200	60

Materials

The materials used in the tests included GLT, concrete, lag screw, and plywood. The GLT is a commonly used engineered material that is assembled, glued, and pressed from laminated wood along the grain direction. The GLT used for wood beam was assigned a strength class of GL26h according to EN 14080 (2013). Following EN 408 (2010) standard, six compression samples and six shear samples of GLT were tested. Referencing EN 383 (2007) standard, six embedment tests were performed using lag screws with a diameter of 16 mm. The mechanical properties of the GLT are summarized in Table 2. The density of GLT was 536.8 kg/m^3, and the measured moisture content was 11.3%. The concrete used for concrete slab was assigned property class as C40 according to GB/T 50081 (2019) standard. Following GB/T 50081 (2019) standard, three 150 mm cubic samples of concrete were fabricated, and tested under compression at the age of 28 days. The steel used for the screws was carbon steel. The screws were assigned property class as 4.8 according to ISO 898-1 (2013). Referencing ISO 898-1 (2013) standard, six steel fasteners with 16-mm diameter were tested under tensile. The mechanical properties of the concrete and the lag screw are indicated in Table 3. According to EN 636 (2003), the technical class of plywood used in the test was F20/10 E60/40.

Table 2. Mechanical Properties of GLT Parallel-to-Grain

Property	Number of Samples	Mean Value (Coefficient of Variation)	Unit
Compressive strength	6	57.3 (4%)	MPa
Compressive elasticity modulus	6	12.57 (3%)	GPa
Shear strength	6	4.28 (4%)	MPa
Embedment strength	6	43.7 (5%)	MPa

Table 3. Mechanical Properties of Concrete and Lag Screws

Material	Property	Number of Samples	Mean Value (Coefficient of Variation)	Unit
Concrete	Compressive strength	3	38.7 (4%)	MPa
Lag screw	Tensile strength	6	461.8 (1%)	MPa
	Yield strength	6	375.4 (1%)	MPa

Test setup and loading method

Shear tests at room temperature were conducted on the composite specimens, as displayed in Fig. 2. The self-balancing frame provided constraints for the end of the GLT beam, and the limit beam effectively reduced the uplifting of the concrete slab. Displacement between the concrete slab and GLT beam was measured by two displacement sensors mounted at each side. The load was applied using the 300-kN hydraulic jack and transferred uniformly through the steel plate to the end of shear specimens.

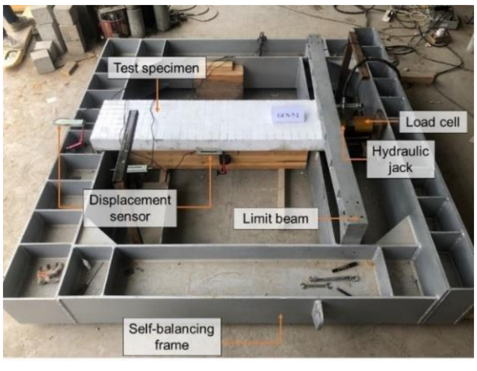

Fig. 2. Shear test setup at room temperature

The loading procedure at room temperature was referred to the EN 26891 (1991) standard. The load was increased with the rate of 20% of the estimated maximum load (F_{est}) per minute until 40% of the maximum load was reached. The load was kept constant for 30 s. Then the load was reduced to $0.1F_{\mathrm{est}}$ and kept constant for 30 s. After that, the load was increased to 0.7 F_{est} in 3 min. Finally, the further load was applied with a displacement-control mode until failure.

Shear tests under fire conditions were performed on a test furnace, which is divided into 3 m × 1.4 m × 1.5 m block by the fireproof brick wall, as displayed in Fig. 3. The furnace could accommodate 4 specimens, each with its own hydraulic jack. Both ends of the concrete slab were propped up on the self-balancing frame and fireproof brick wall respectively. Both ends of the GLT beam were propped up on the fire-resistant cotton and the fireproof brick wall. Two draw-wire displacement sensors were placed on the hydraulic jack at each side, and their wires were fastened to the H-section steel. The load was applied from the 300-kN hydraulic jack and transferred uniformly through the H-section steel to the end of the shear specimens to keep the jack away from fire.

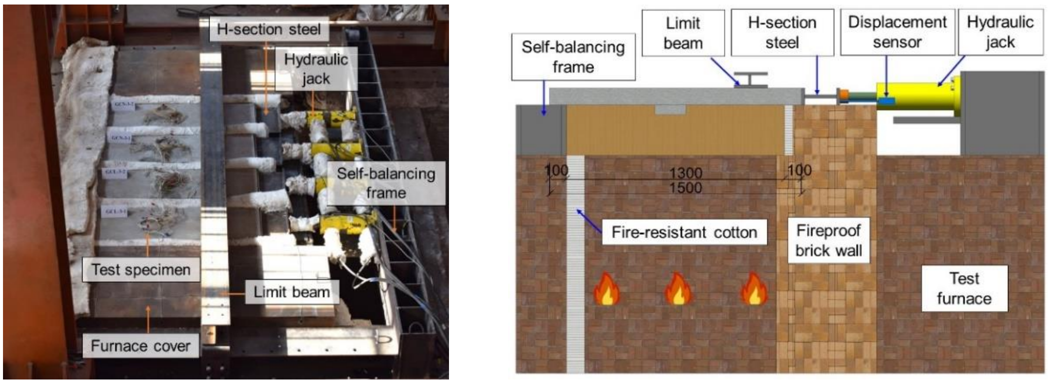

a) b)

Fig. 3. Shear test setup under fire conditions (unit: mm): a) top view; and b) side view

The loading procedure under fire conditions was based on the shear tests under ISO 834-1 (2012) standard fire conditions performed by Fontana and Frangi (1999), *i.e.*, specimens were subjected to fire under a steady load, namely 10% of maximum load at room temperature. If the specimens did not fail during the fire duration, then the supply of natural gas was cut off and the load was increased at a rate of 0.5 kN/s until failure. The fire temperature-time relationship of ISO 834-1 (2012) used in the tests, is shown in Eq. 1,

$$T=345\log_{10}(8t+1)+20 \tag{1}$$

where T is the average furnace temperature (°C), t is the time (min).

RESULTS AND DISCUSSION

Experimental Observations

At room temperature

Figure 4 indicates the typical failure mode of the specimens at room temperature. When the load approached to 0.6 $F_{\max}$, small cracks began to appear on the top surface of the concrete slab. An obvious gap could be observed between the concrete slab and the GLT beam when the load was close to 0.9 $F_{\max}$. After reaching the ultimate load, the shear failure occurred of the notched concrete specimen (Fig. 4a). After the screw was pulled out, it was found that the screw formed one plastic hinge on the contact surface of concrete and

GLT, and another plastic hinge in the concrete sheared plane (Fig. 4a). Apart from the different number of plastic hinges for the lag screws, there were no noticeable differences in failure modes among the GCN150-AT, GCN200-AT (Fig. 4b), and GCN250-AT specimens.

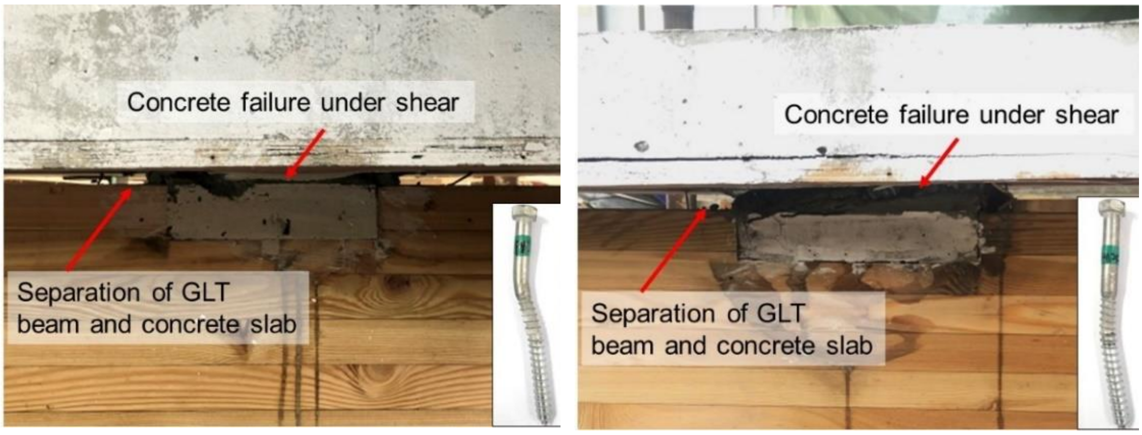

a) **b)**

Fig. 4. Shear failure of the notched concrete and the gap between components: a) GCN150-AT; and b) GCN200-AT

Under ISO fire conditions

Figure 5 indicates two types of failure modes for the specimens under fire conditions. After the tests, for four experimental groups (GCN200-ET30, GCN200-ET45, GCN200-ET60, and GCN250-ET45), no failure of notched concrete was observed. After the concrete slab and plywood of the specimen were removed, it was found that the notched wood suffered compression failure, and the wood around the hole was obviously deformed (Fig. 5a). After the screw was pulled out, it was found that, for compression failure of wood, the screw possibly formed a plastic hinge at the vertical contact between the concrete and the GLT (Fig. 5a). The final failure of the GCN150-ET45 specimen was different from other specimens, as a crack was observed to develop along the notch length (Fig. 5b). The reduction of the notch length to 150 mm reduced the concrete sheared plane, and the failure mode of the specimen changed from the compression failure of wood to the shear failure of concrete.

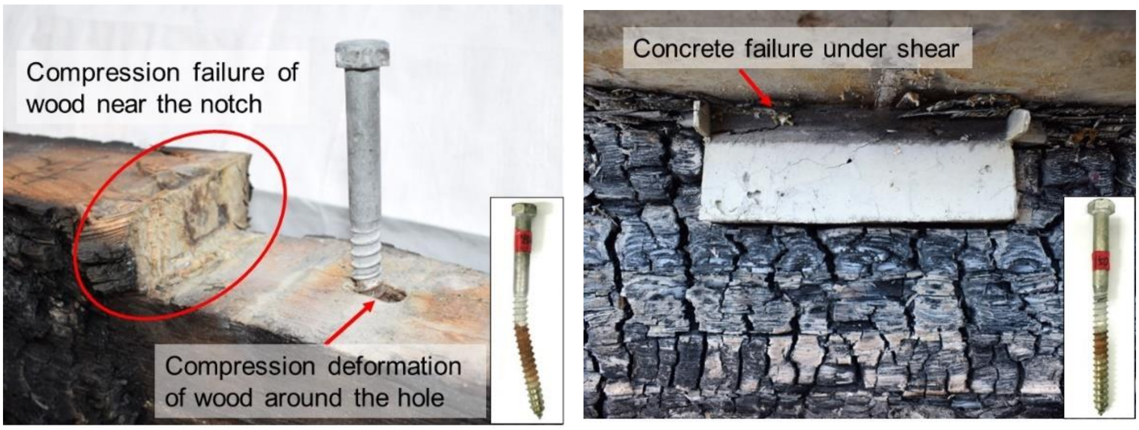

a) **b)**

Fig. 5. Failure modes of shear specimens under fire conditions: (a) compression deformation of notched wood and the hole (GCN200-ET45); and (b) concrete failure under shear (GCN150-ET45)

Test Results

Figure 6 displays the load-slip relationships of the shear specimens with different parameters. The load-slip relationships of specimens at room temperature could be roughly divided into three parts based on the slope change (Fig. 6a). In the first part, the curves under load rose linearly, and the concrete sheared plane was not fully formed. In the second part, the curves rose non-linearly, and the slope of the curves decreased. The main reason for this part could be the local shear cracking of the notched concrete, which led to the reduction of shear stiffness of the connectors. In the third part, the load promptly dropped because of brittle shear failure of the notched concrete.

The load-slip relationships of specimens under fire could be roughly divided into three parts as well (Fig. 6b). In the first part, specimens were loaded to the constant load, and the curves rose linearly before fire. After the load stabilized, the furnace was turned on and the specimens were exposed to fire. Under constant load, the displacement increments during fire were small. The specimens were exposed to fire but did not fail. For the second part, the furnace was turned off at the beginning and the load increased. The curves rose non-linearly, and the slip stiffness was degraded. The main reason for this part could be that at this stage, when the furnace was turned off and the load was increased, the specimens shear stiffness decreased after being exposed to fire. In the third part, the curves descended, and the descent speed decelerated until the specimens failed completely.

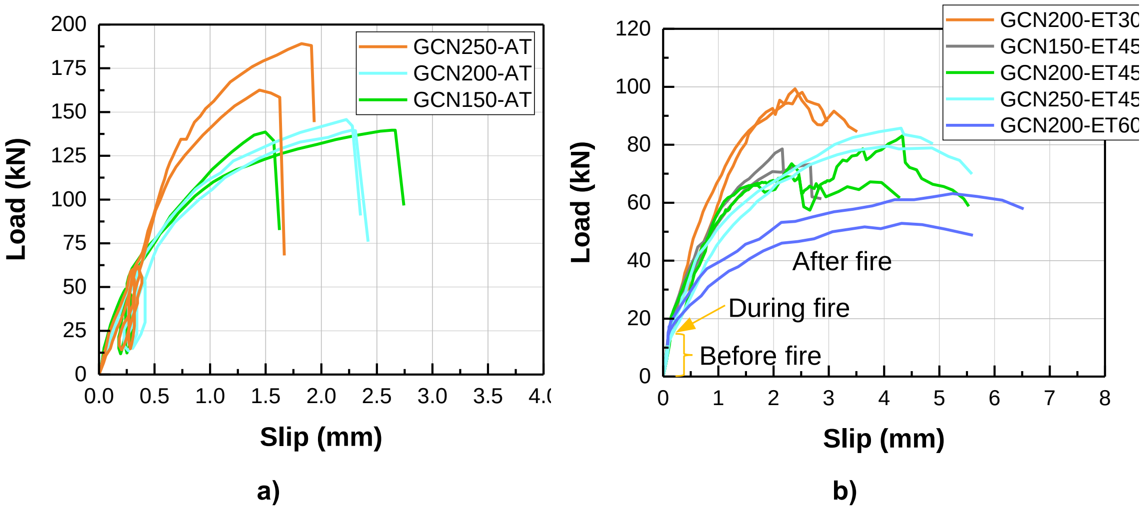

Fig. 6. Load-slip relationships of shear specimens: a) at room temperature; and b) under fire conditions

The shear test results of the specimens at room temperature and fire conditions are indicated in Table 4. The average residual width and height of wood beams in the area near to the notch after the fire exposure are shown in Table 4. The ultimate load F_{max}, the slip value at ultimate load $v_{F_{max}}$, the slip value at 40% ultimate load $v_{0.4}$, and the slip value at 10% ultimate load $v_{0.1}$ are defined following EN 26891 (1991). The serviceability slip modulus K_s, which represents the deformation resistance of the shear connectors, is calculated by Eq. 2:

$$K_s = \frac{0.4F_{max}}{4/3(v_{0.4} - v_{0.1})} \tag{2}$$

Table 4. Results Obtained from Shear Tests at Room Temperature and Fire Conditions

Specimen Group	Number of Specimens	Fire Duration (min)	Residual width (mm)	Residual height (mm)	K_s (kN/mm)	$v_{F_{max}}$ (mm)	F_{max} (kN)	Failure Mode
					Average Values			
GCN150-AT	2	0	-	-	176.13	2.07	139.12	S
GCN200-AT	2	0	-	-	175.01	2.26	141.70	S
GCN250-AT	2	0	-	-	179.38	1.63	175.83	S
GCN150-ET45	2	45	89	268	57.83	2.41	75.93	S
GCN200-ET45	2	45	86	267	58.92	3.34	78.28	C
GCN250-ET45	2	45	89	270	61.19	4.59	82.28	C
GCN200-ET30	2	30	110	279	88.79	2.46	98.71	C
GCN200-ET60	2	60	76	242	37.52	4.78	58.01	C

Note: S denotes shear failure of notched concrete; C denotes compression failure of notched wood

Discussion

The effects of fire duration ranging from 30 to 60 min on the shear performance of notched connectors are described in Table 4. Compared with the GCN200-AT specimen, the shear stiffness of the GCN200-ET30 specimen were reduced by 49%, that of the GCN200-ET45 specimen were reduced by 66%, and that of the GCN200-ET60 specimen were reduced by 79%. The increase in fire exposure time reduced effective width of the notched wood, negatively affected the shear stiffness and bearing capacity of the notched connectors, where the shear stiffness decreased more rapidly.

The effects of notch length ranging from 150 to 250 mm on the shear stiffness of notched connectors are described in Table 4. At room temperature, the shear stiffness of the GCN150-AT, GCN200-AT, and GCN250-AT specimens were similar, because the high stiffness of notched connectors mainly came from the compression area of the notched concrete and notched wood. The notch length had little effect on the connector shear stiffness. Under fire conditions, the shear stiffness of the GCN150-ET45, GCN200-ET45, and GCN250-ET45 specimens were similar as well, because the fire duration was the same and the remaining compression area was similar.

Prediction of Shear Stiffness for Notched Connectors

At room temperature

In Table 5, the effects of concrete strength, notch length, notch width, timber sheared length, and steel fasteners on the notched connectors shear stiffness can be observed. From the experimental results of Yeoh *et al.* (2008), Thai *et al.* (2020), and Jiang *et al.* (2020), it can be concluded that screw diameter, screw length, and the presence of a screw did not noticeably affect the connectors' shear stiffness within the investigated range. The research data of Yeoh *et al.* (2008) and Jiang *et al.* (2020) showed that timber sheared length had little influence on the connectors' shear stiffness. The experimental results from this study suggested that the variation of notch length between 150 and 250 mm did not remarkably affect the connectors' shear stiffness. The research data of Yeoh *et al.* (2008) and Shi *et al.* (2022) indicated that with increased notch width, the stiffness of notched connectors had an obvious increasing trend.

Table 5. Shear Stiffness of Notched Connectors Obtained from Experiments

Author	Specimen	l_n (mm)	t_n (mm)	b_n (mm)	l_{ts} (mm)	Timber Type E_t (GPa)	f_c (MPa)	d (mm); l_s (mm)	$K_{s,t}$ (kN/mm)
This study	GCN150-AT	150	40	150	550	GLT; 12.70	38.7	16; 195	176.13
	GCN200-AT	200							175.01
	GCN250-AT	250							179.38
Yeoh *et al.* (2008)	A1	150	50	63	300	LVL; 11.34	45	16; 200	80.20
	B1			63	300		45	-	104.70
	C1			63	300		45	12; 200	77.90
	F1			63	200		45	16; 200	92.70
	G1			63	300		42.7	16; 200	67.00
	H1			126	200		45	16; 200	217.90
Jiang *et al.* (2020)	NC-N-1	150	50	150	350	GLT; 10.68	29.2	-	229.62
	LC-N-1				350		28.7	-	234.38
	LC-NS-1				150		28.7	16; 200	231.84
	LC-NS-2				200		28.7	16; 200	247.35
	LC-NS-3				275		28.7	16; 200	239.05
	LC-NS-4				350		28.7	16; 200	249.40
Shi *et al.* (2022a)	RSS (C)	150	50	135	150	GLT; 12.90	42.8	16; 190	273.80
	RDS *			135			42.8		259.70
	HRSS			85			40.8		158.90
	HRSS (R) **			85			40.8		169.00
Thai *et al.* (2020)	C *	200	35	200	400	CLT; 11.70	36.8	8; 160	248
	D *	200			400			8; 220	238
	G *	300			300			8; 160	208
	H *	300			300			8; 220	195
	L *	250			350			8; 220	205
Zhang *et al.* (2020b)	L-40-250	150	40	200	250	GLT; 12.00	52	-	233.40

Note: l_n, t_n, b_n are length, depth, and width of the notch, respectively; l_{ts} is the timber sheared length; E_t is the elasticity modulus of timber; f_c is the concrete compressive strength; d is the diameter of the steel fastener; and l_s is the overall length of the steel fastener.
* Double fasteners in the notch
** Two additional reinforcement fasteners (d = 7 mm, l_s = 140 mm) for timber

The high stiffness of the notched connectors is largely due to the compressive contact between the wood and concrete on the effective bearing surface. Zhang *et al.* (2022a,b) conducted experimental and theoretical analyses on notched connectors and concluded that shear stiffness of reinforced and non-reinforced connectors was similar under the serviceability limit state. They proposed that the shear stiffness of 1-m width notched connector is approximately $2.5E_t t_n$ kN/mm. Then the shear stiffness of notched connectors with notch width of b_n can be calculated using Eq. 3,

$$K_s = 2.5E_t t_n (b_n / w) \tag{3}$$

where K_s is the connector stiffness under serviceability limit state (kN/mm), E_t is the elasticity modulus of timber (GPa), t_n is the notch depth (mm), b_n is the notch width (mm), and w = 1 m.

The application of Eq. 3 needs to satisfy the following: (1) The notch has a rectangular geometric shape with the notch depth t_n of 35 to 50 mm, the notch length l_n of 150 to 250 mm, and the timber sheared length l_{ts} of 150 to 550 mm; (2) The timber types can be GLT, LVL, and cross-laminated timber (CLT) or other parallel laminated wood products with uniform lamination properties; (3) The elasticity modulus of wood E_t ranges from 6 to 15 GPa, and the elasticity modulus of concrete ranges from 15 to 45 GPa

(Zhang *et al.* 2022c). Under the above conditions, calculation results of Eq. 3 were compared with experimental results of this study and other researchers, as shown in Table 6. The maximum deviation between the calculated stiffness and the measured stiffness was 26%, and most of the calculated values showed deviations within ± 20%, indicating good agreement.

Table 6. Comparison of Experimental and Calculation Results of Shear Specimens at Room Temperature

Author	Specimen	$K_{s,t}$ (kN/mm)	$K_{s,c}$ (kN/mm)	$K_{s,t}/K_{s,c}$
This study	GCN150-AT	176.13	188.55	0.93
	GCN200-AT	175.01	188.55	0.93
	GCN250-AT	179.38	188.55	0.95
Yeoh *et al.* (2008)	A1	80.20	89.30	0.90
	B1	104.70	89.30	1.17
	C1	77.90	89.30	0.87
	F1	92.70	89.30	1.04
	G1	67.00	89.30	0.75
	H1	217.90	178.61	1.22
Jiang *et al.* (2020)	NC-N-1	229.62	200.25	1.15
	LC-N-1	234.38	200.25	1.17
	LC-NS-1	231.84	200.25	1.16
	LC-NS-2	247.35	200.25	1.24
	LC-NS-3	239.05	200.25	1.19
	LC-NS-4	249.40	200.25	1.25
Shi *et al.* (2022a)	RSS (C)	273.80	217.69	1.26
	RDS	259.70	217.69	1.19
	HRSS	158.90	138.13	1.15
	HRSS (R)	169.00	138.13	1.22
Thai *et al.* (2020)	C	248	204.75	1.21
	D	238	204.75	1.16
	G	208	204.75	1.02
	H	195	204.75	0.95
	L	205	204.75	1.00
Zhang *et al.* (2020b)	L-40-250	233.40	240.00	0.97
Mean value				1.08
Coefficient of variation (%)				13.22
Note: $K_{s,t}$ is the measured shear stiffness; $K_{s,c}$ is the calculated shear stiffness				

Under ISO fire conditions

An increase of wood temperature negatively affected the effective compression area between the notched wood and notched concrete, the elasticity modulus of the wood, and the connectors shear stiffness. Therefore, notched connectors shear stiffness for GLT-concrete composite beams under ISO fire was calculated, considering that the elasticity modulus of the notched wood, and the effective compression area decreased with the rise of temperature.

According to the numerical model from Shi *et al.* (2022b), the temperatures of the notched wood were higher than that of the wood with the same fire-exposed distance. The temperature of the notched wood can be calculated as,

$$\Theta_{\mathrm{i}}(x,y) = 20 + 180(\beta t)^{\alpha}\left\{\left(\frac{1}{x}\right)^{\alpha} + \left(\frac{1}{b_{\mathrm{t}} - x}\right)^{\alpha} + \left(\frac{1}{y}\right)^{\alpha}\right\} \tag{4}$$

$$\alpha = \begin{cases} 0.01t + 1.55 \text{for } 0 < t \leq 30 \\ 0.016t + 1.65 \text{for } 30 < t \leq 45 \\ 0.022t + 1.75 \text{for } 45 < t \leq 60 \end{cases} \quad (5)$$

where Θ_i is the temperature (°C) of timber beam that depends on its width x and height y, β is the charring rate of timber beam (mm/min), t is the fire exposure time (min), x, y is the distance from original exposed surface (mm), b_t is the beam width (mm), and α is the exponent determined by Eq. 5.

As shown in Fig. 7, the notched wood was divided into rectangular elements i with a width of 3 mm. The elasticity modulus of wood was assumed to drop to zero at temperatures above 300 °C (EN 1995-1-2, 2003). Then, the width of wood at temperatures below 300 °C was the effective notch width b_{ef}. The mean temperature of the element $\theta_{mean, i}$ was calculated by Eq. 4, and the elasticity modulus of the element under fire $E_{t, i}(\theta_{mean, i})$ was calculated from reduction factor of elasticity modulus of wood according to EN 1995-1-2 (2003). Finally, all elements were integrated to calculate the shear stiffness of notched connectors under fire conditions, as proposed in Eq. 6,

$$K_{s, fi} = 2.5t_n \sum_{i=1}^{n} [E_{t, i}(\theta_{mean, i}) \Delta b_{ni} / w] \quad (6)$$

where $K_{s, fi}$ is the connector stiffness after fire exposure (kN/mm), $E_{t, i}(\theta_{mean, i})$ is the elasticity modulus of timber calculated from element mean temperature (GPa), and Δb_{ni} is the element width of the notched wood (mm).

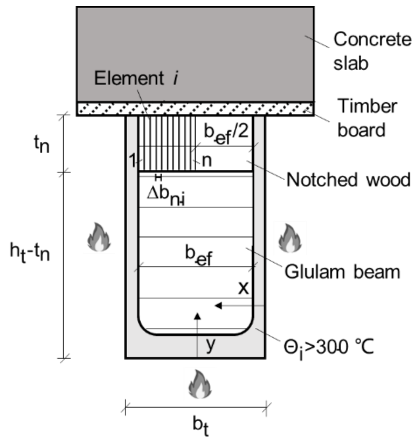

Fig. 7. Element *i* of the notched wood

Table 7. Comparison of Experimental and Calculated Results of Shear Specimens Under Fire Conditions

Specimen Group	Number of Specimens	$K_{s, t, fi}$(kN/mm)	$K_{s, c, fi}$(kN/mm)	$K_{s, t, fi}/K_{s, c, fi}$
GCN150-ET45	2	57.83	50.24	1.15
GCN200-ET45	2	58.92	50.24	1.17
GCN250-ET45	2	61.19	50.24	1.22
GCN200-ET30	2	88.79	73.58	1.21
GCN200-ET60	2	37.52	31.77	1.18
Mean Value				1.19
Coefficient of Variation (%)				2.43
Note: $K_{s, t, fi}$ is the measured shear stiffness of connectors after fire; $K_{s, c, fi}$ is the calculated shear stiffness of connectors after fire				

As indicated in Table 7, the calculated results are above the measured results, with a maximum deviation of 22%, which can conservatively predict the notched connectors shear stiffness under fire.

CONCLUSIONS

1. Under fire conditions, the reduction of the notch length from 200 to 150 mm when the wood sheared length was 550 mm remarkably affected the failure mode of the shear specimens, changing from compression failure of notched wood to shear failure of notched concrete.
2. The increase in fire duration reduced the effective width of the notched wood. It negatively affected the shear stiffness and bearing capacity of the notched connectors, where the shear stiffness decreased more rapidly. The notch length did not noticeably affect the notched connectors shear stiffness. This was because changes in the notch length did not affect the wood sheared area; *i.e.*, wood sheared length was always set to 550 mm independently of the notch length. For shorter wood sheared length, results may vary, and further testing is required.
3. Based on the temperature distributions of the notched wood, an analytical model for conservatively predicting the notched connectors shear stiffness of the GLT-concrete composite beam under fire conditions was established.

ACKNOWLEDGEMENTS

The research was supported by National Natural Science Foundation of China (Nos. 51678295 and51478220).

REFERENCES CITED

Auclair, S. C. (2020). *Design Guide for Timber-Concrete Composite Floors in Canada*, FPInnovations, Pointe-Claire, Quebec, Canada.

Ceccotti, A. (2002). "Composite concrete-timber structures," *Progress in Structural Engineering and Materials* 4(3), 264-275. DOI: 10.1002/pse.126

Dias, A., Lopes, S., Van de Kuilen, J., and Cruz, H. (2007). "Load-carrying capacity of timber-concrete joints with dowel-type fasteners," *Journal of Structural Engineering* 133(5), 720-727. DOI: 10.1061/(ASCE)0733-9445(2007)133:5(720)

Dias, A., and Jorge, L. (2011). "The effect of ductile connectors on the behaviour of timber–concrete composite beams," *Engineering Structures* 33(11), 3033-3042. DOI: 10.1016/j.engstruct.2011.05.014

Dias, A., Schänzlin, J., and Dietsch, P. (2018). *Design of Timber-Concrete Composite Structures* (COST Action FP1402/WG 4), European Cooperation in Science and Technology (COST), Brussels, Belgium.

Djoubissie, D., Messan, A., Fournely, E., and Bouchair, A. (2018). "Experimental study of the mechanical behavior of timber-concrete shear connections with threaded reinforcing bars," *Engineering Structures* 172, 997-1010. DOI: 10.1016/j.engstruct.2018.06.084

Du, H., Hu, X., Xie, Z., and Wang, H. (2019). "Study on shear behavior of inclined cross lag screws for glulam-concrete composite beams," *Construction and Building Materials* 224, 132-143. DOI: 10.1016/j.conbuildmat.2019.07.035

Du, H., Hu, X., Wang, H., Zhang, J., and Sun, Z. (2020). "Shear performance of inclined screws in glulam-concrete composite beams," *Journal of Building Structures* 41(7), 191-200. DOI: 10.14006/j.jzjgxb.2018.0739

Du, H., Hu, X., Xie, Z., and Meng, Y. (2021a). "Experimental and analytical investigation on fire resistance of glulam-concrete composite beams," *Journal of Building Engineering* 44, article ID 103244. DOI: 10.1016/j.jobe.2021.103244

Du, H., Hu, X., Han, G., and Shi, D. (2021b). "Experimental and analytical investigation on flexural behaviour of glulam-concrete composite beams with interlayer," *Journal of Building Engineering* 38, article ID 102193. DOI: 10.1016/j.jobe.2021.102193

EN 383 (2007). "Timber structures – Test methods – Determination of embedding strength and foundation values for dowel type fasteners," European Committee for Standardization, Brussels, Belgium.

EN 408 (2010). "Timber structures – Structural timber and glued laminated timber – Determination of some physical and mechanical properties," European Committee for Standardization, Brussels, Belgium.

EN 1995-1-2 (2003). "Eurocode 5: Design of timber structures – Part 1-2: General rules– Structural fire design," European Committee for Standardization, Brussels, Belgium.

EN 26891 (1991). "Timber structures – Joints made with mechanical fasteners – General principles for the determination of strength and deformation characteristics," European Committee for Standardization, Brussels, Belgium.

EN 14080 (2013). "Timber structures – Glued laminated timber and glued solid timber – Requirements," European Committee for Standardization, Brussels, Belgium.

EN 636 (2003). "Plywood – Specifications," European Committee for Standardization, Brussels, Belgium.

Fontana, M., and Frangi, A. (1999). "Fire behaviour of timber-concrete composite slabs," in: *5th World Conference on Timber Engineering, Proceedings*, Presses Polytechniques et Universitaires Romandes, Montreux, Switzerland, Vol. 1, pp. 76-83.

Frangi, A., Knobloch, M., and Fontana, M. (2010). "Fire design of timber-concrete composite slabs with screwed connections," *Journal of Structural Engineering* 136(2), 219-228. DOI: 10.1061/(ASCE)ST.1943-541X.0000101

GB/T 50081 (2019). "Standard for test methods of concrete physical and mechanical properties," Standardization Administration of China, Beijing, China.

ISO-834-1:1999/Amd1:2012 (2012). "Fire-resistance tests – Elements of building construction – Part 1: General requirements," International Organization for Standardization, Geneva, Switzerland.

ISO 898-1 (2013). "Mechanical properties of fasteners made of carbon steel and alloy steel – Part 1: Bolts, screws and studs with specified property classes – Coarse thread and fine pitch thread," International Organization for Standardization, Geneva, Switzerland.

Jiang, Y., and Crocetti, R. (2019). "CLT-concrete composite floors with notched shear connectors," *Construction and Building Materials* 195, 127-139. DOI: 10.1016/j.conbuildmat.2018.11.066

Jiang, Y., Hu, X., Hong, W., Zhang, J., and He, F. (2020). "Experimental study on notched connectors for glulam- lightweight concrete composite beams," *BioResources* 15(2), 2171-2180. DOI: 10.15376/biores.15.2.2171-2180

Kavaliauskas, S., Kvedaras, A. K., and Valiūnas, B. (2007). "Mechanical behaviour of timber-to-concrete connections with inclined screws," *Journal of Civil Engineering and Management* 13(3), 193-199. DOI: 10.3846/13923730.2007.9636437

Marchi, L., and Pozza, L. (2021). "Timber-concrete composite connections using GFRP notches fastened with self-tapping screws: Conceiving, numerical modelling and testing," *Construction and Building Materials* 294, article ID 123579. DOI: 10.1016/j.conbuildmat.2021.123579

Shi, B., Dai, Y., Tao, H., and Yang, H. (2022a). "Shear performances of hybrid notch-screw connections for timber-concrete composite structures," *BioResources* 17(2), 2259-2274. DOI: 10.15376/biores.17.2.2259-2274

Shi, D., Hu, X., Du, H., Meng, Y., and Xie, Z. (2022b). "Thermo-mechanical analysis on shear behavior of grooved connectors for glulam-concrete composite beams under fire," *Fire Safety Journal* 130, article ID 103594. DOI: 10.1016/j.firesaf.2022.103594

Thai, M. V., Ménard, S., Elachachi, S. M., and Galimard, P. (2020). "Performance of notched connectors for CLT-concrete composite floors," *Buildings* 10(7), article no. 122. DOI: 10.3390/buildings10070122

Xie, Z., Hu, X., Du, H., and Zhang, X. (2020). "Vibration behavior of timber-concrete composite floors under human-induced excitation," *Journal of Building Engineering* 32, article ID 101744. DOI: 10.1016/j.jobe.2020.101744

Yeoh, D., Fragiacomo, M., Aldi, P., Mazzilli, M., and Kuhlmann, U. (2008). "Performance of notched coach screw connection for timber-concrete composite floor system," *NZ Timber Design Journal* 17(1), 4-10.

Yeoh, D., Fragiacomo, M., and Deam, B. (2011a). "Experimental behaviour of LVL–concrete composite floor beams at strength limit state," *Engineering Structures* 33(9), 2697-2707. DOI: 10.1016/j.engstruct.2011.05.021

Yeoh, D., Fragiacomo, M., De Franceschi, M., and Buchanan, M. (2011b). "Experimental tests of notched and plate connectors for LVL-concrete composite beams," *Journal of Structural Engineering* 137(2), 261-269. DOI: 10.1061/(ASCE)ST.1943-541X.0000288

Zhang, J., Hu, X., Hong, W., Li, L., and Sun, Q. (2020a). "Experimental study on seismic performance of subassemblages between glulam-concrete composite beam and glulam column," *Journal of Building Structures* 41(1), 131-148. DOI: 10.14006/j.jzjgxb.2018.0557

Zhang, L., Chui, Y., and Tomlinson, D. (2020b). "Experimental investigation on the shear properties of notched connections in mass timber panel-concrete composite floors," *Construction and Building Materials* 234, article ID 117375. DOI: 10.1016/j.conbuildmat.2019.117375

Zhang, X., Hu, X., Gong, H., Zhang, J., Lv, Z., and Hong, W. (2020c). "Experimental study on the impact sound insulation of cross laminated timber and timber-concrete composite floors," *Applied Acoustics* 161, article no. 107173. DOI: 10.1016/j.apacoust.2019.107173

Zhang, L., Zhou, J., and Chui, Y. (2022a). "Development of high-performance timber-concrete composite floors with reinforced notched connections," *Structures* 39, 945-957. DOI: 10.1016/j.istruc.2022.03.074

Zhang, L., Zhou, J., Chui, Y., and Tomlinson, D. (2022b). "Experimental investigation on the structural performance of mass timber panel-concrete composite floors with notched connections," *Journal of Structural Engineering* 148(2), article ID 04021249. DOI: 10.1061/(ASCE)ST.1943-541X.0003229

Zhang, L., Zhou, J., Zhang, S., and Chui, Y. (2022c). "Bending stiffness prediction to mass timber panel-concrete composite floors with notched connections," *Engineering Structures* 262, article ID 114354. DOI: 10.1016/j.engstruct.2022.114354

Article submitted: July 22, 2022; Peer review completed: September 3, 2022; Revised version received: September 16, 2022; Accepted: September 26, 2022; Published: September 28, 2022.
DOI: 10.15376/biores.17.4.6397-6410